Quantum Monte Carlo calculations on open shell species inside helium clusters

Marius Lewerenz

Quantum Monte Carlo calculations on open shell species inside helium clusters

Marius Lewerenz
Laboratoire de Modélisation et Simulation Multi Echelle
UMR8208 CNRS
Université Paris Est (Marne la Vallée)
5, Blvd. Descartes, Champs sur Marne
77454 Marne la Vallée Cedex 2
France

Acknowledgments

Paris-Est:
Ji Jiang, Ph.D student, $Ar^+@He_n$, $I^q@He_n$
Mirjana Mladenović, $CO^+@He_n$

Prague:
Petr Slavíček, $Pb^{q+}@He_n$

ANR project DYNHELIUM (Toulouse, Rennes, Paris)

What makes helium clusters interesting?

- Helium-helium interaction is of weak van der Waals type, closed shell atoms of very low polarisability, $D_e \approx 7.6\ cm^{-1}$
- Helium atoms have a relatively small mass.
- Large zero point energy effects (D_0 for $He_2 \approx 0.001\ cm^{-1}$).
- Helium clusters are small chunks of a quantum liquid.
- Quantum statistical effects: bosonic ^4He, fermionic ^3He.
- Superfluidity in bulk liquid ^4He below 2.17 K, in ^3He at mK level
- A very special solvent: Is there a new chemistry?

- Implantation of dopants through (multiple) inelastic collisions.
- Weak interactions with dopant.
- Binding energy and position of dopants depend on quantum effects.

Delicate balance between potential and quantum kinetic energy

Plenty of interesting experiments but theoretical difficulties!

Recent applications of helium clusters

- Matrix spectroscopy with minimal perturbations: OCS, $(HF)_n$, biomolecules at 0.4 K, radicals
- Reaction dynamics at very low temperatures: $Ba + N_2O \rightarrow BaO + N_2$
- Preparation of reactive intermediates: $HF \cdots CH_3$, $HCN \cdots CH_3$ etc.
- Preparation of high spin metal polymers: Na_3, K_3, Rb_3 etc.
- Assembly of cold clusters: Ag_n, Mg_n
- Thermodynamically unstable isomers: linear $(HCN)_n$
- Nanomodels for molecule-surface interactions: $HCN \cdots Mg$ etc.

- Container for soft ionisation for analytical mass spectrometry?
- Energy dissipation by coupling to the bath?
- Confinement medium for cluster ignition and Coulomb explosion.
- Spacer for interatomic Coulombic decay (ICD).

A typical helium droplet experiment

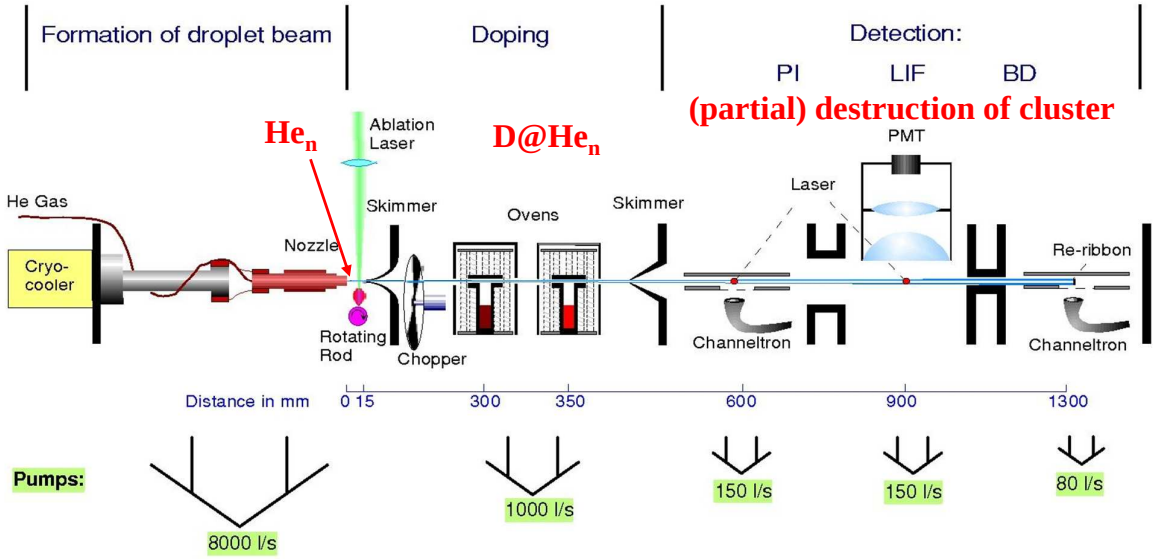

Observation of ionic clusters resulting from fragmentation or ejected photo fragments

$I@He_n$ from $CH_3I \rightarrow CH_3 + I.$

Experimental fragment distributions vs. ab initio+diffusion quantum Monte Carlo results

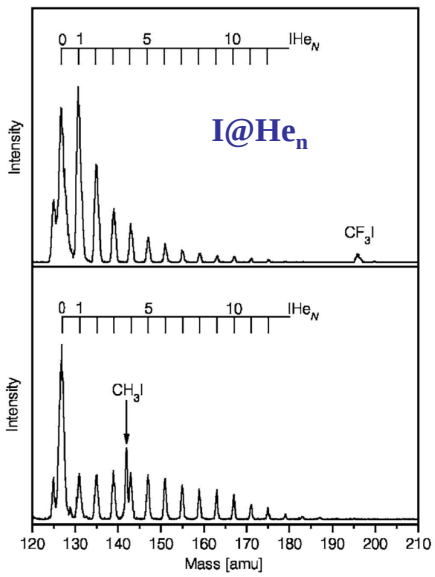

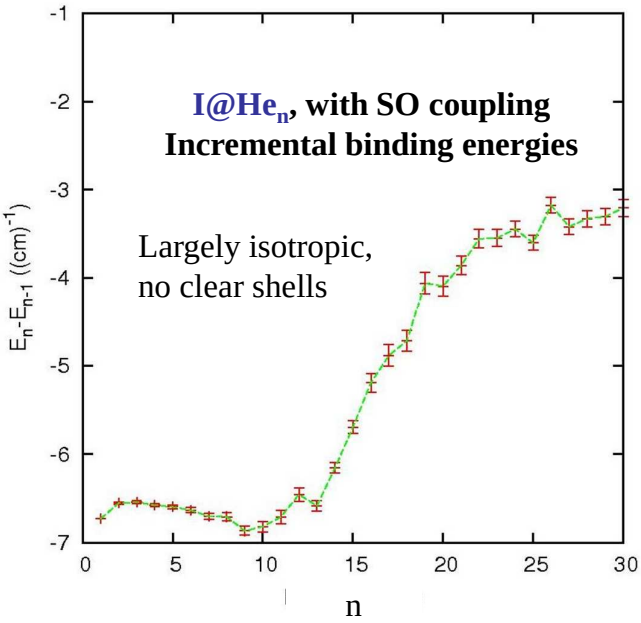

Braun and Drabbels 2007

Pair potentials involving helium and metals

Shallower well than He-He and larger equilibrium distance for He-M

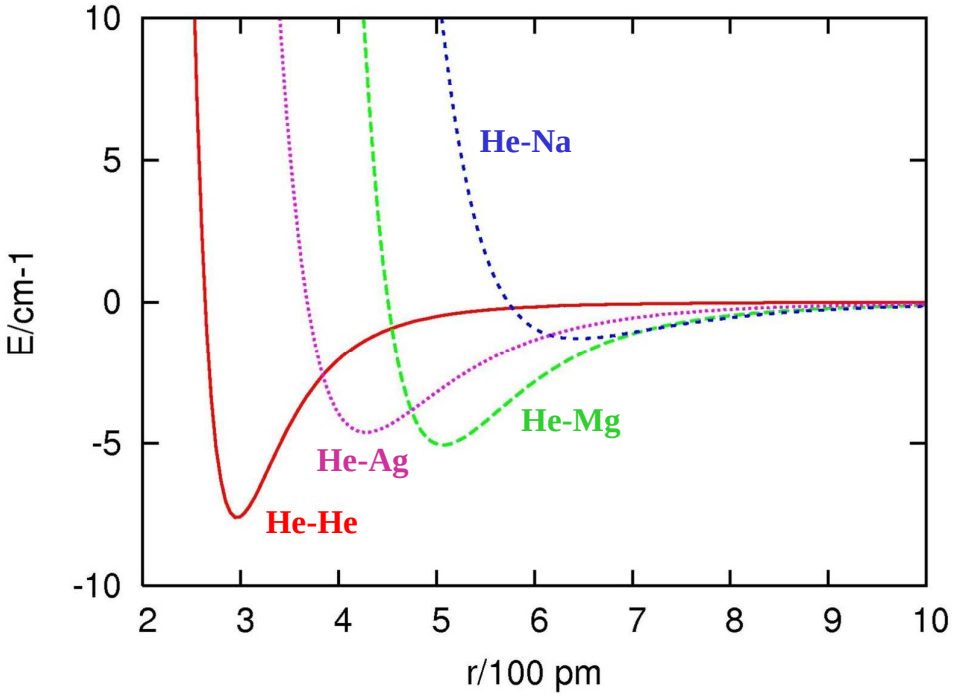

Ions in helium clusters

- **Massive change of interaction potential**
- **Polarisation forces**
- **Enhanced localisation of helium atoms**
- **"Snowball" formation**

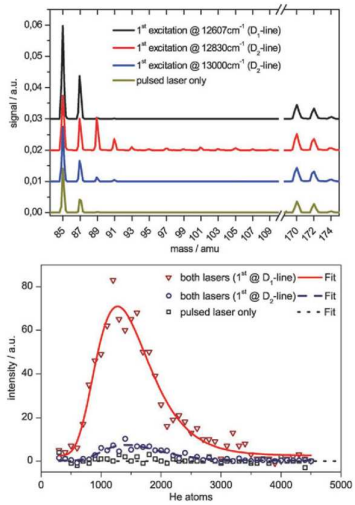

PCCP **Two step photoionisation Theisen et al., TU Graz**

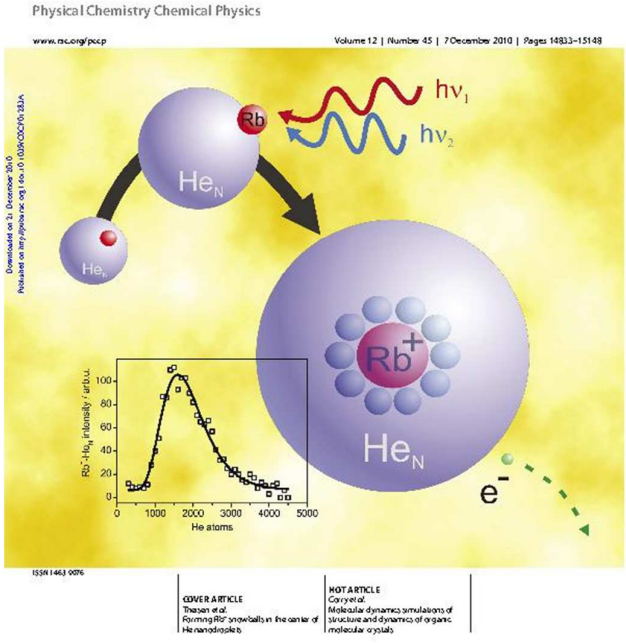

Modelling open shell species inside helium clusters

ANR project DYNHELIUM (Paris , Rennes, Toulouse):

Dissociation, recombination/caging and/or cluster exit of reaction products

Our ultimate test problem, well known in the gas phase:

Photodissociation of $CH_3I \rightarrow CH_3 + I$ inside He_n

We need global potential energy surfaces for ground and excited $CH_3I@He_n$ and for the relevant fragments $CH_3@He_n$ and $I@He_n$ (electronic anisotropy!).

Isoelectronic warm up system:

Ar^+ ions (s^2p^5 valence shell, $X^2\Sigma^+$ and $A^2\Pi$ states for Ar^+He).
Spin-orbit coupling between Σ and Π states has to be included in the model.
Spin-orbit splitting is typically larger than the van der Waals interaction:
Δ = 1432 cm^{-1} for Ar^+, Δ = 7600 cm^{-1} for I

Include non additive induced dipole – induced dipole interaction for charged species

Diffusion quantum Monte Carlo (DMC)

- Isomorphism between time dependent Schrödinger equation and a multi dimensional diffusion equation (Fermi, Ulam)
- Exact solution except for statistical errors

$$\imath\hbar\frac{\partial\Psi(\vec{r},t)}{\partial t} = \left\{-\frac{\hbar^2}{2}\sum_{j=1}^{n}\frac{1}{m_j}\nabla_j^2 + \{V(\vec{r}) - E_{ref}\}\right\}\Psi(\vec{r},t)$$

?

$$\frac{\partial C(\vec{r},t)}{\partial t} = \left\{\sum_{j=1}^{n} D_j\nabla_j^2 - k(\vec{r})\right\}C(\vec{r},t)\ .$$

Solution by propagation of an ensemble of random walkers in imaginary time
Cartesian coordinates, precision $\sigma_E/E = 10^{-6} – 10^{-3}$

DMC calculations for Ar^+He_n

Potential model:

Anisotropy due to Ar^+ s^2p^5 valence shell → $X^2\Sigma^+$ and $A^2\Pi$ states for Ar^+He.

IP(Ar)=15.76 eV → He^++Ar channel is unimportant, single configuration.
RCCSD(T) calculations with (aug)-cc-pVXZ basis sets (MOLPRO).

Infinite basis set ab initio points fitted to HFD-style analytical form with fixed C_4 coefficient computed from α_{He} = 1.41 a_0^3.

Strong spin-orbit interaction in Ar^+ (Δ = 1432 cm^{-1}):
Non additive many body potential model including induced dipoles on He with additional spin-orbit mixing included using atomic Δ_{Ar+} (complex 6 x 6 matrix to diagonalise in each DMC step).

Ar^+He: convergence of interaction energy

RCCSD(T) calculation, standard and augmented basis sets

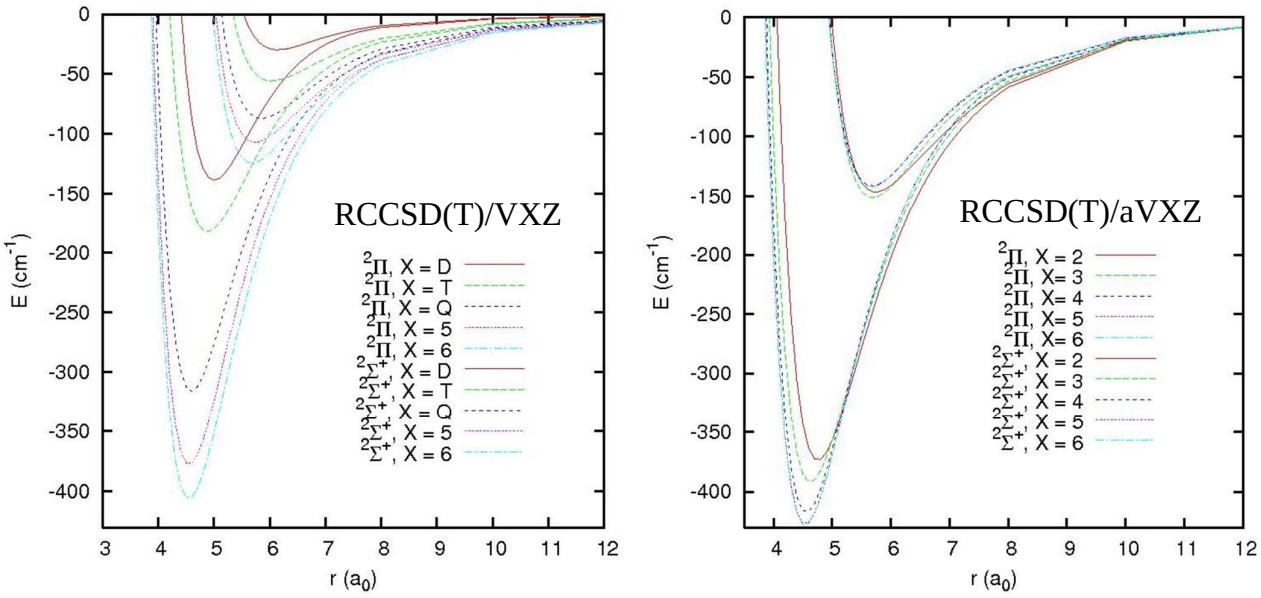

Ar^+He: spectroscopic observables

CCSD(T), infinite basis extrapolated potentials (aQ56), atomic Δ_{so}, variational rovibrational calculation in Laguerre basis, $^4He^{40}Ar^+$

Vibrational transition frequencies in cm-1

v	$X\ ^2\Sigma^+_{1/2}$			$A_1\ ^2\Pi_{3/2}$		$A_2\ ^2\Pi_{1/2}$		
	exp	S96	This work	S96	This work	exp	S96	This work
0	**92.9**	83.9	**92.47**	52.9	55.91	**69.2**	64.0	**69.19**
1	**66.2**	55.2	**64.88**	26.9	29.20		35.1	38.82
2		30.7	38.55	11.9	11.73		15.7	17.59
3		14.1	17.81					

Expectation values for rotational constants in cm-1

0	**0.659**	0.614	**0.650**	0.460	0.469	**0.515**	0.501	**0.514**
1	**0.551**	0.518	**0.559**	0.355	0.365	**0.420**	0.397	**0.412**
2	**0.39**	0.404	**0.450**	0.241	0.255		0.282	0.298
3		0.282	0.324	0.168	0.087		0.182	0.180
4		0.182	0.196					

Our Ar^+He potential is excellent !

Ar^+He_n : DMC ground state energies vs. exp.

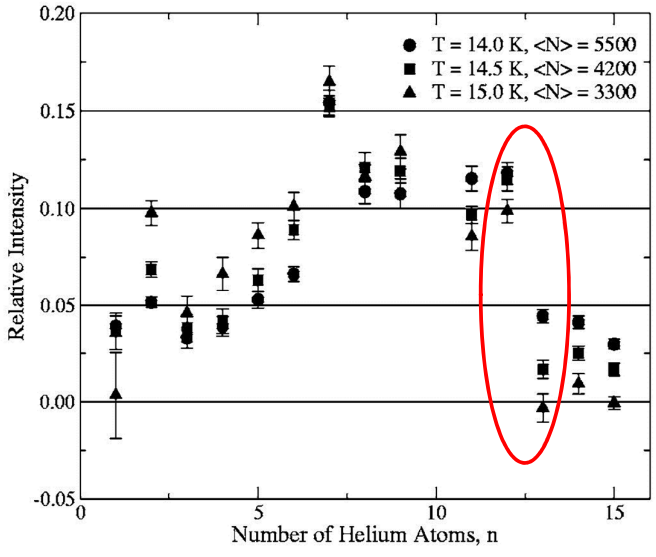

Fragmentation after ionisation of $Ar@He_N$, Brindle et al. 2005

Energy increments

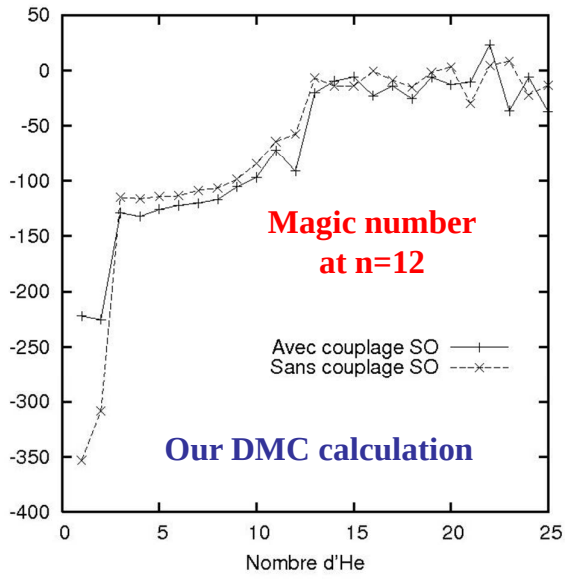

Spin orbit coupling is responsible for magic character of n=12 cluster

DMC calculations for $I@He_n$

Motivation: **Photodissociation of $CH_3I \rightarrow CH_3 + I$ inside He_n.**
We need global potential energy surfaces for ground and excited $CH_3I@He_n$ and for the relevant fragments $CH_3@He_n$ and $I@He_n$

Potential model:

Anisotropy due to I s^2p^5 valence shell → $X^2\Sigma^+$ and $A^2\Pi$ states for I-He.
RCCSD(T) calculations with aug-cc-pVXZ basis sets and relativistic pseudopotential (ECP) from K. Petersen.

Ab initio points fitted to extended Tang-Toennies analytical form.

Very strong spin-orbit interaction in I:
Non additive many body potential model with additional spin-orbit mixing using atomic Δ_I (complex 6 x 6 matrix to diagonalise in each DMC step).

Δ_{SO} dominates so much over E_{vdW} that SO mixing is almost perfect!

I-He: Convergence of RCCSD(T)/ECP calculations

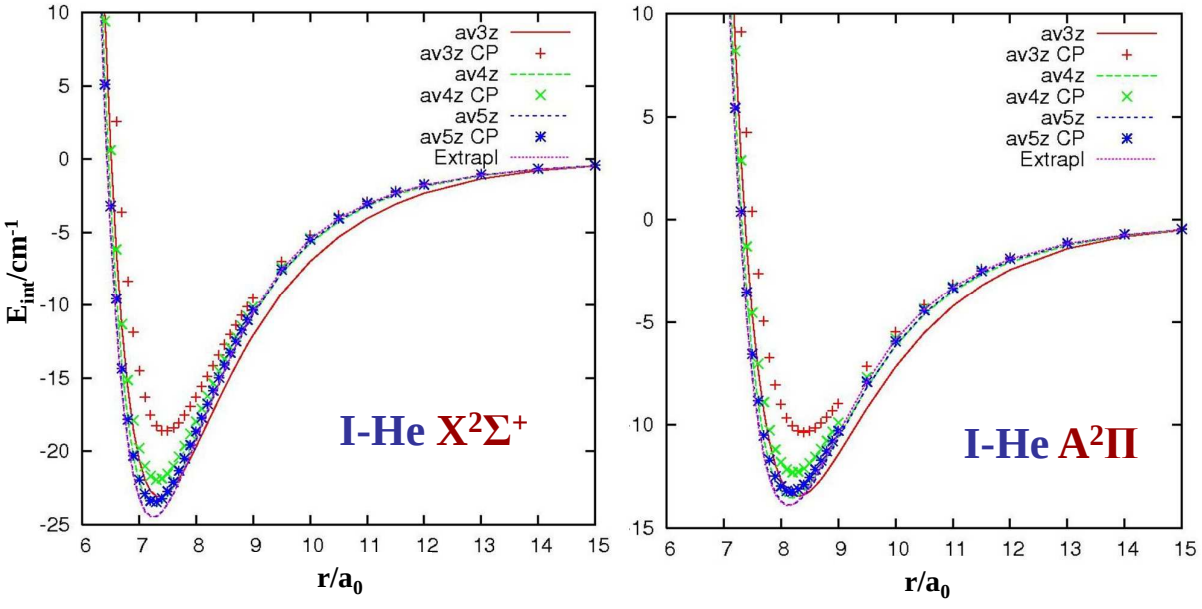

Spin-orbit coupling mixes the $^2\Sigma_{1/2}$ and $^2\Pi_{1/2}$ components: 6x6 complex matrix

I-He: Interaction potential with SO coupling

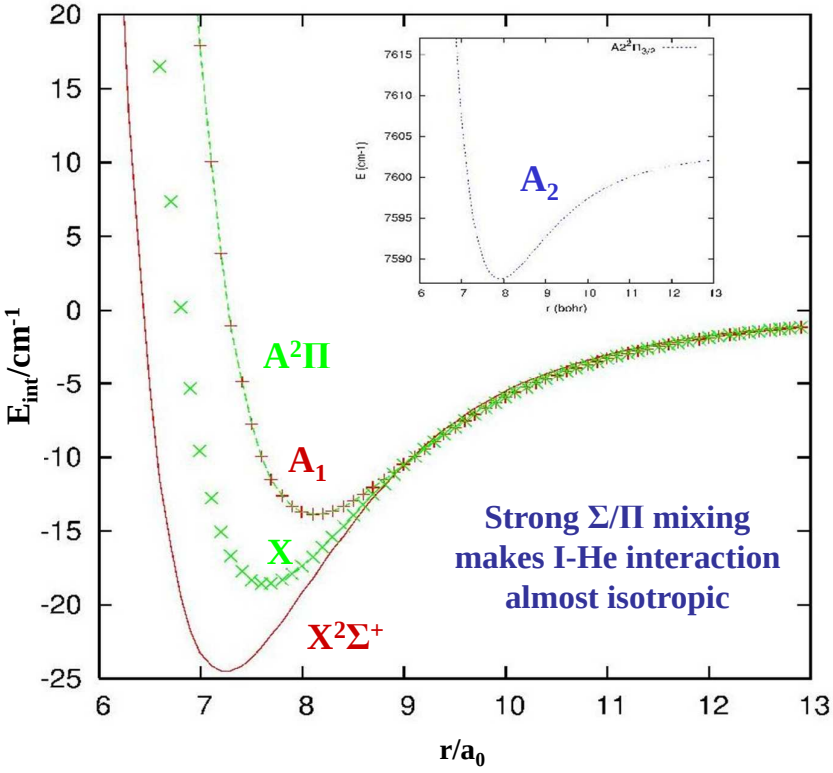

RCCSD(T), small core ECP, MOLPRO code, infinite basis extrapolation, experimental atomic SO constant.

$I@He_n$: Radial helium density from DMC

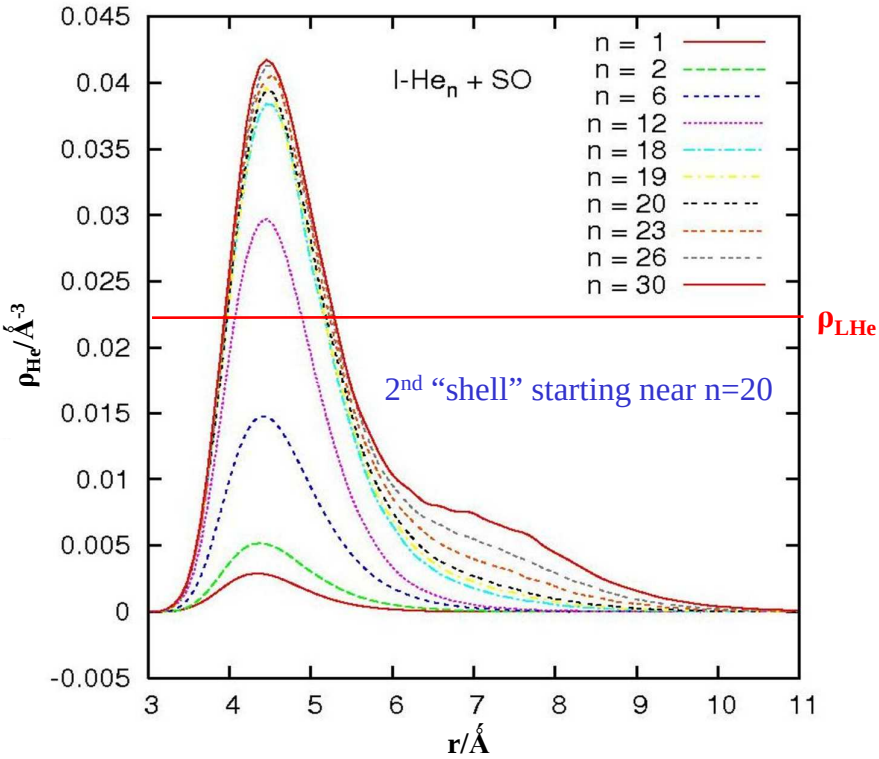

$I@He_n$: Incremental binding energies from DMC

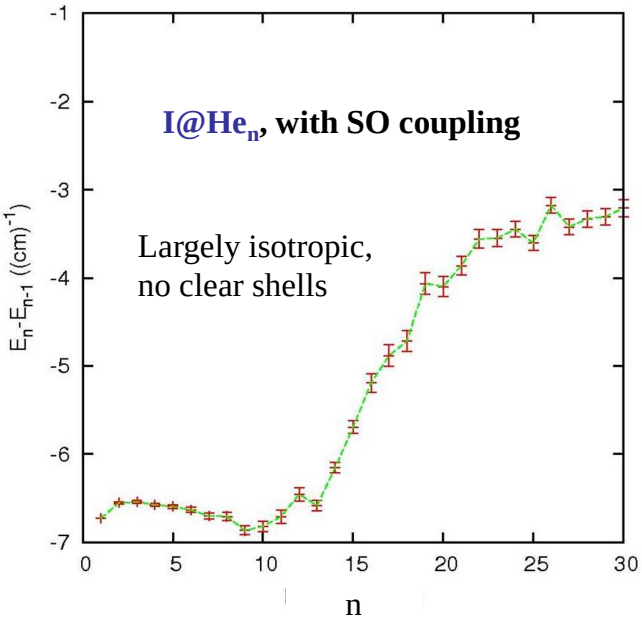

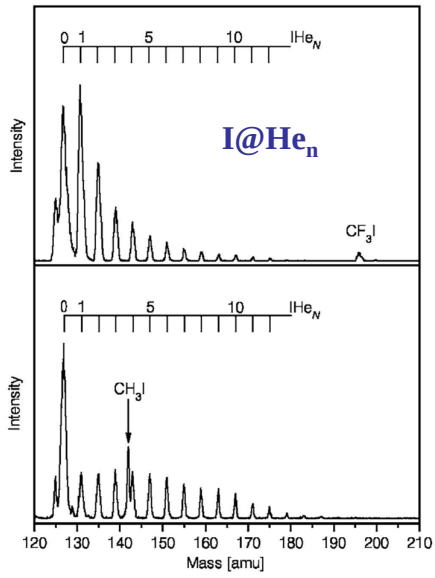

Braun and Drabbels 2007

$I^-@He_n$: Binding energy and radial helium density

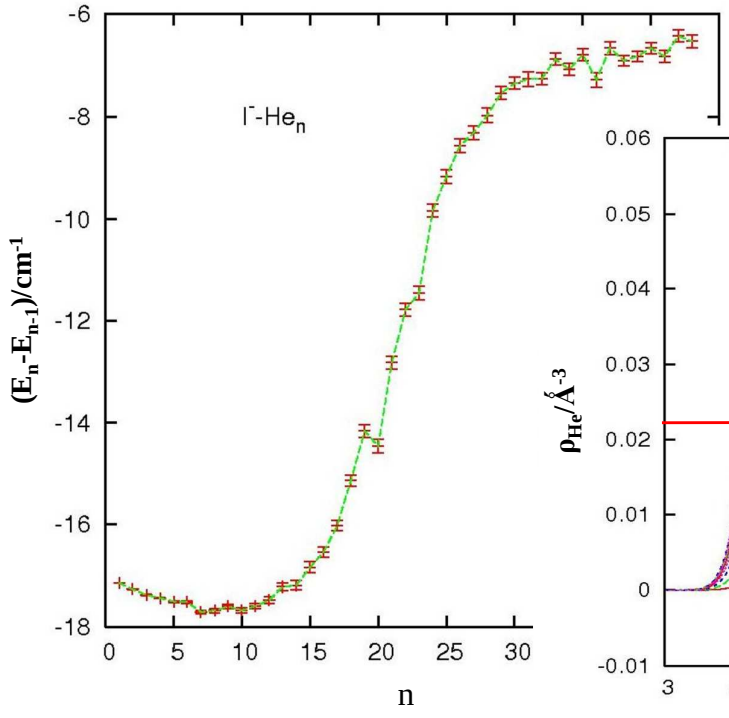

Soft transition to
2nd "shell" near n=25

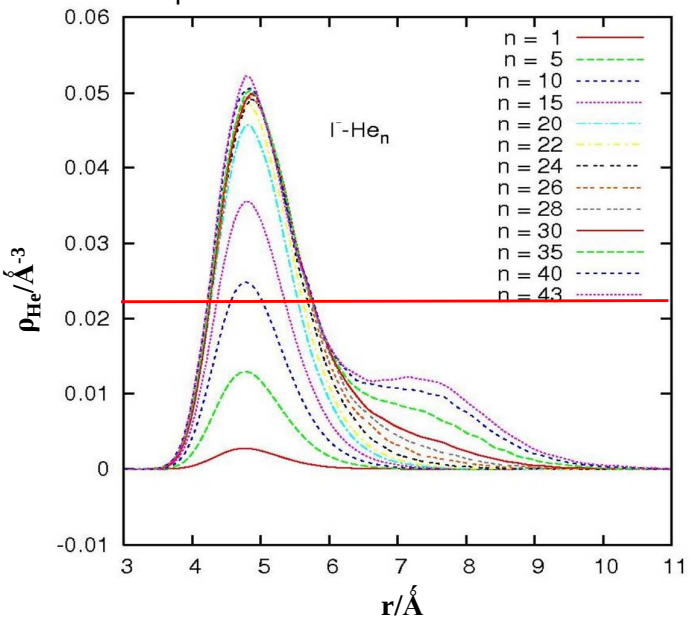

$I^-@He_n$: Angular correlations

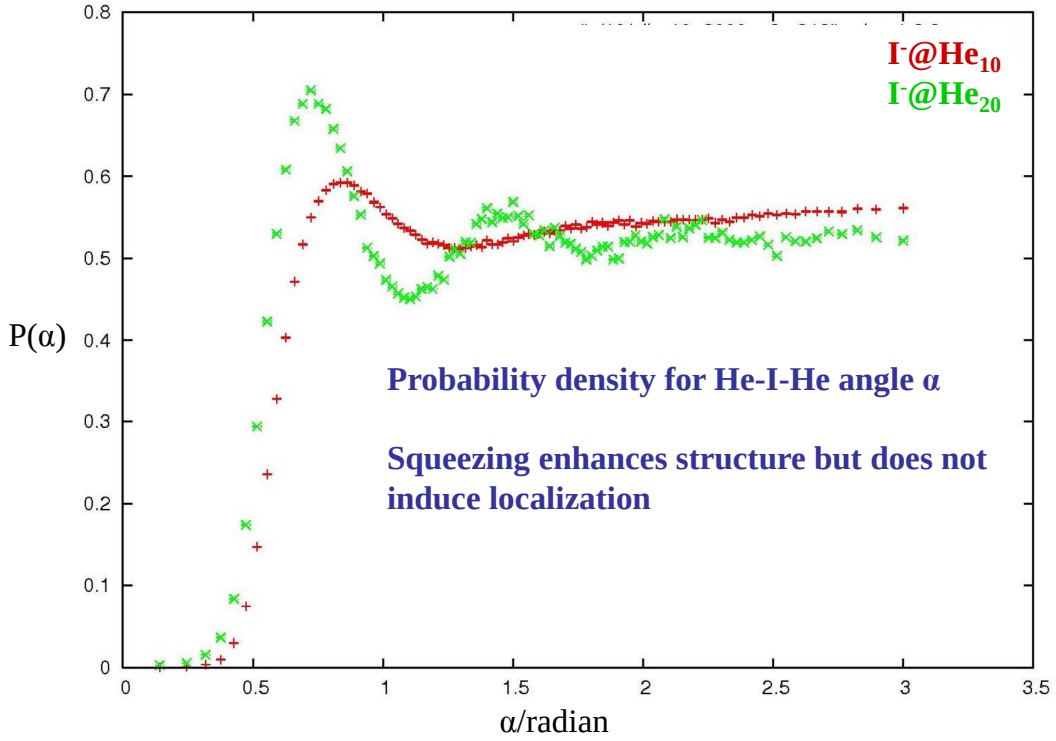

$I^{2+}@He_n$: Binding energy and radial helium density

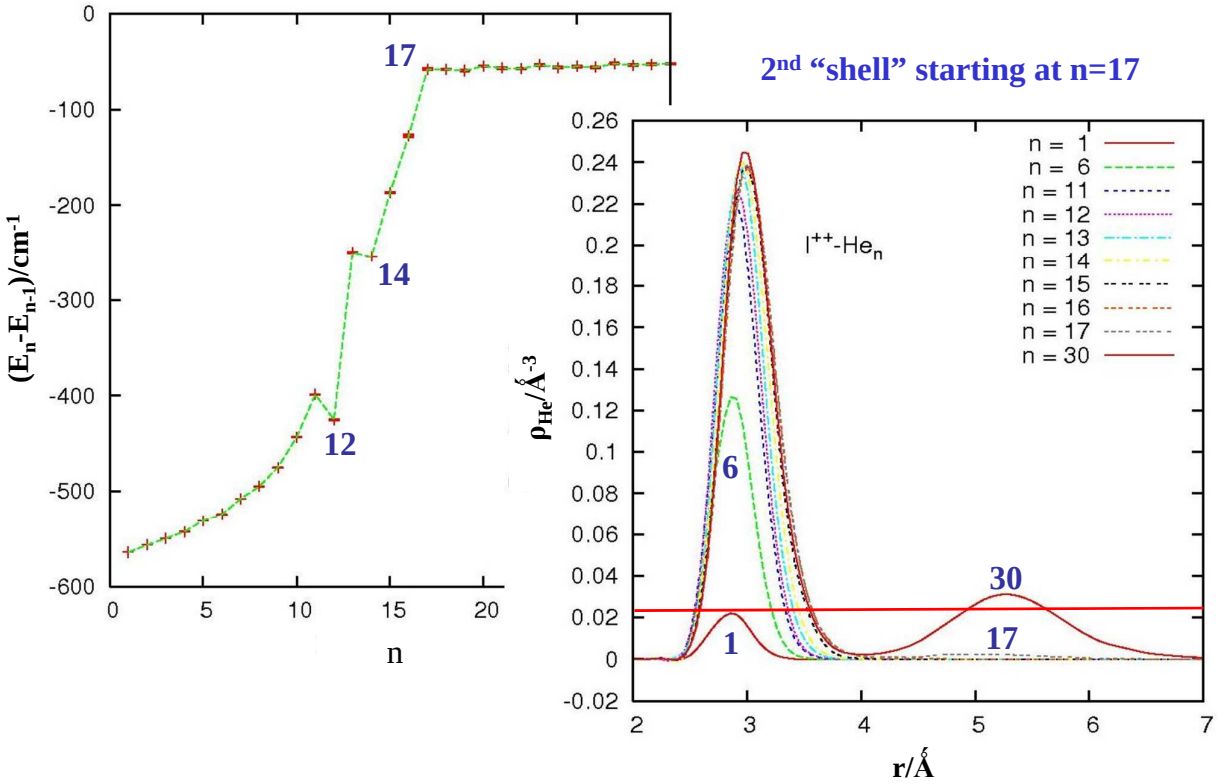

CO^+-He and $CO^+@He_n$

Evidence for formation of CO^+He ions in several drift tube experiments.
No experimental spectroscopic information.
Mixed cluster ions of the composition CO^+He_n should be accessible in drift tube experiments, mixed gas expansions coupled to electric discharges, or CO ionization inside large He clusters.

Ionisation of CO barely changes the rotational constants but strongly affects the interaction with helium: $CO@He_n$ and CO^+He_n are an ideal pair to understand rotation in helium clusters by separating effects due to mass and interaction.

Potential surface can be checked by ion depletion spectroscopy (see N_2^+-He_n).

Astrophysical motivation

CO is rather abundant in interstellar space and CO^+ has been identified in 1993. Low energy collisions with helium atoms, its second most abundant and non reactive collision partner, are governed by the weak intermolecular interaction leading to the van der Waals complex $He\text{-}CO^+$.

Features of the CO^+-He surface

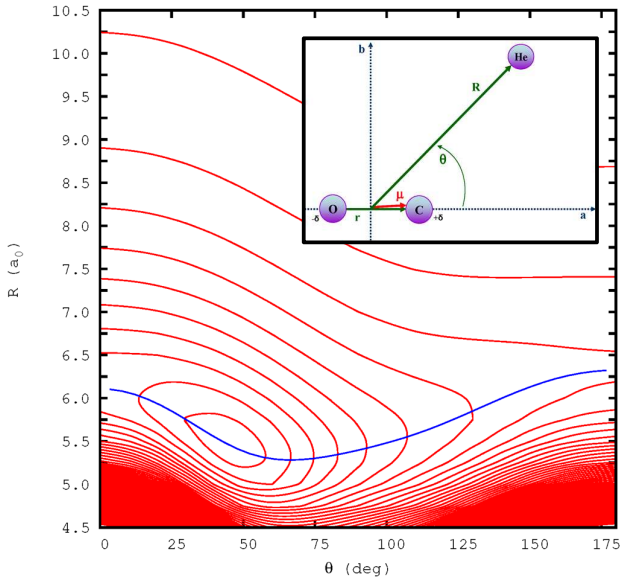

2D contour plot of the RCCSD(T) PES.
Contour lines at intervals of 25 cm^{-1}, first contour placed at -250 cm^{-1}. The blue line shows the variation of the Jacobi distance R along the minimum energy path in the direction of the Jacobi angle θ.

RCCSD(T) surface extrapolated to complete basis set limit.

V_{min} = -275.3 cm^{-1}
E_0 = -195.0 cm^{-1}

A_0 = 7.168 cm^{-1}
B_0 = 0.466 cm^{-1}
C_0 = 0.411 cm^{-1}

Quasilinear molecule with strong permanent dipole moment and strong IR transition moment.

Low energy scattering resonance.

Spectroscopic results from DVR-DGB calculations

He-$CO^+(X^2\Sigma^+)$ 2D RCCSD(T) potential energy surfaces V(R,θ) at r(CO)=1.11783 Å

	avtz	avtz$_{corr}$	avqz	avqz$_{corr}$	av5z	av5z$_{corr}$	av∞z
R_e/Å	2.898	2.905	2.870	2.878	2.868	2.871	2.866
θ_e/deg	43.8	46.2	45.8	46.0	46.1	46.1	46.3
V_{min}/cm^{-1}	-285.8	-252.4	-281.6	-269.0	-277.7	-274.0	-275.3
E_0/cm^{-1}	-209.7	-177.5	-201.3	-189.9	-197.6	-194.2	-195.0
A_0/cm^{-1}	10.3	7.315	7.679	7.328	7.362	7.256	7.168
B_0/cm^{-1}	0.444	0.454	0.462	0.462	0.465	0.465	0.466
C_0/cm^{-1}	0.395	0.400	0.408	0.407	0.410	0.409	0.411
ν_2/cm^{-1}	31.9	32.8	34.3	34.4	34.7	34.7	34.9
ν_3/cm^{-1}	94.8	86.5	94.2	91.3	93.6	92.8	93.3
Δ_1/cm^{-1}	0.049	0.055	0.056	0.055	0.055	0.055	0.056
κ	-0.990	-0.984	-0.985	-0.984	-0.984	-0.984	-0.983
γ_0	-0.31	0.08	0.08	0.12	0.12	0.14	0.15

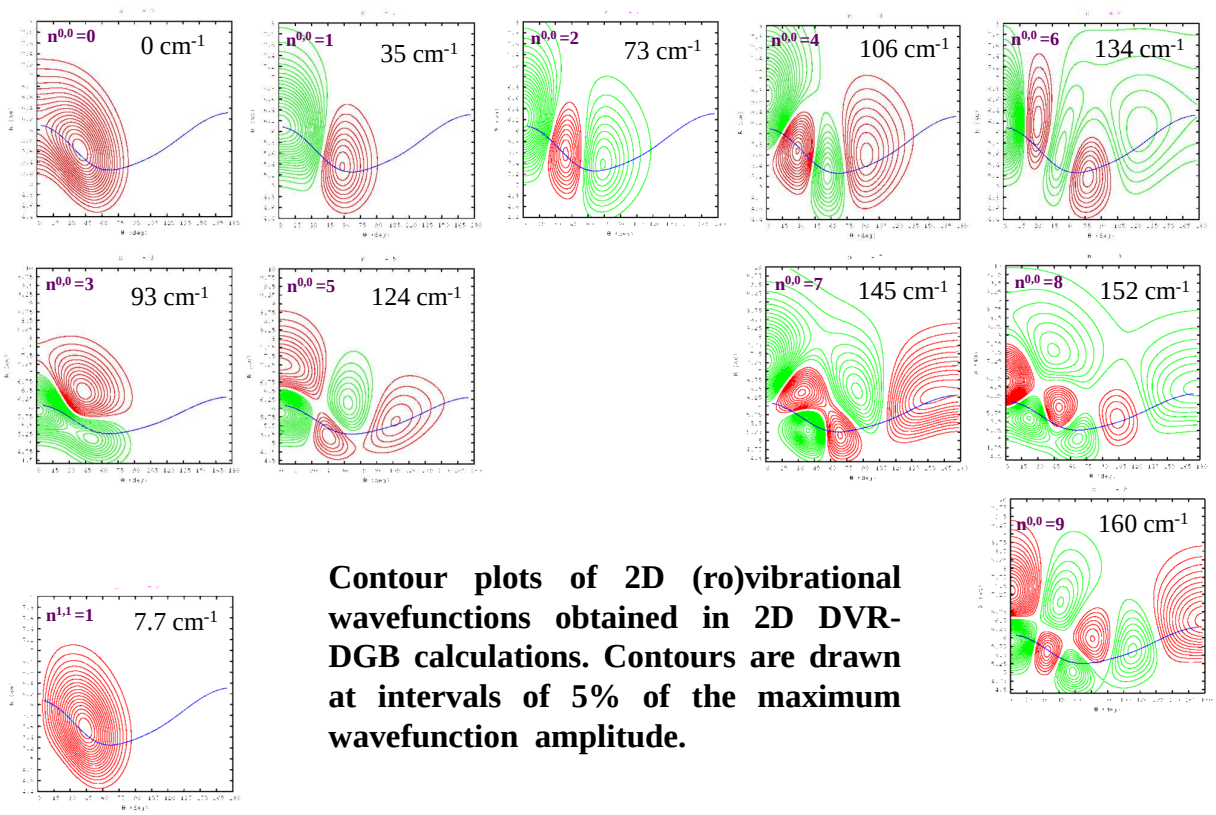

Contour plots of 2D (ro)vibrational wavefunctions obtained in 2D DVR-DGB calculations. Contours are drawn at intervals of 5% of the maximum wavefunction amplitude.

CO^+-He ground state as seen by DMC:

He density histogram in cylinder coordinates (z,r)

O→C defines z-axis, origin at c.o.m. of CO unit

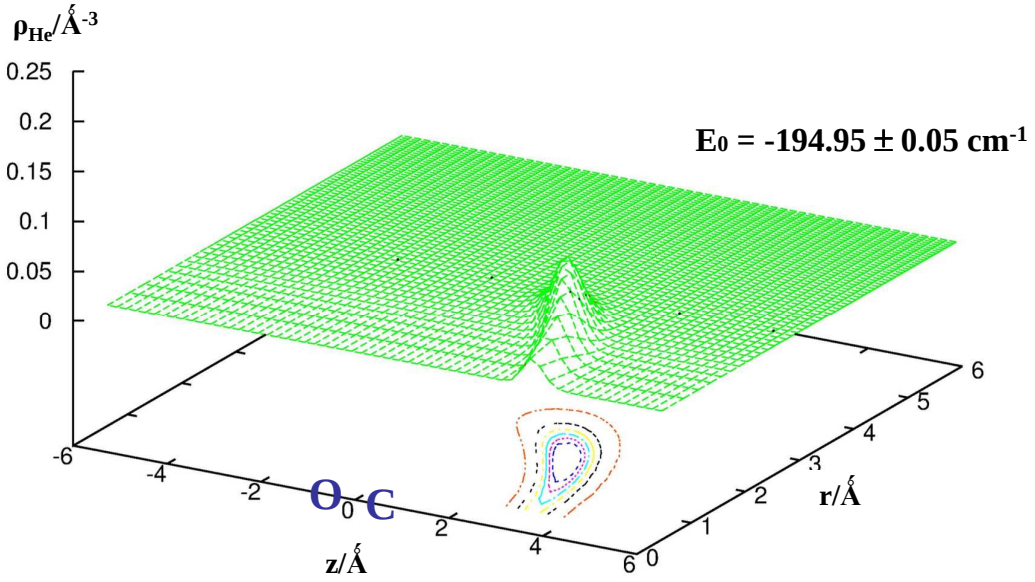

Contour lines at ρ_{He} = 0.001, 0.01, 0.02, 0.03, 0.04, 0.05, 0.1, 0.15, 0.20, 0.25 Å^{-3}

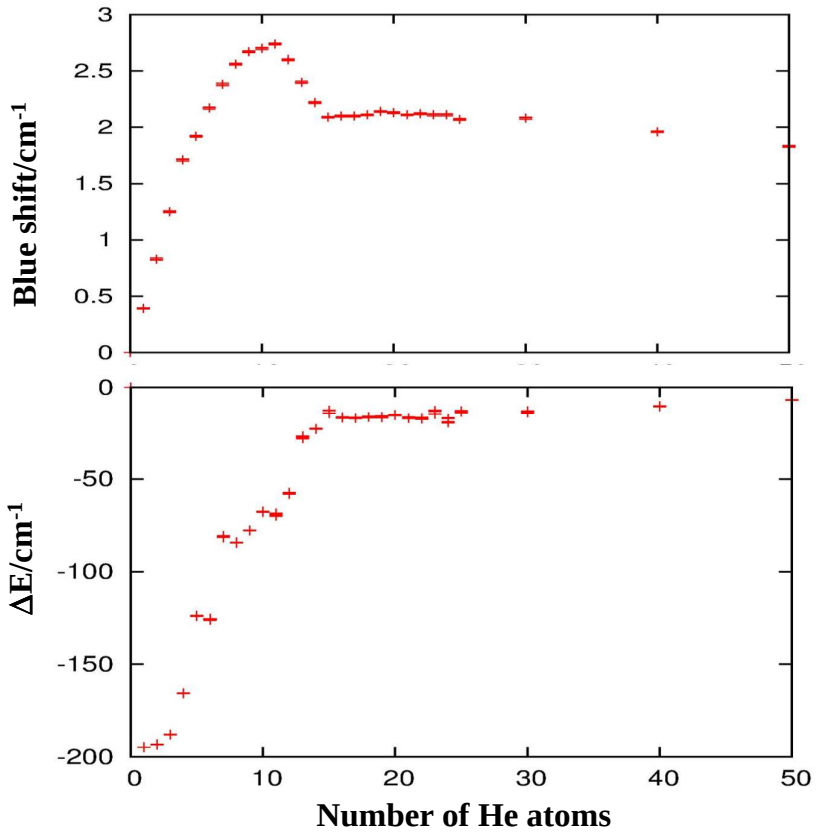

$CO^+@He_n$

Energy increments ΔE (chemical potential, bottom graph) and CO^+ frequency shift (upper graph) from adiabatic method (intermolecular potential as parametric function of the CO^+ vibrational state). Many body model with induced dipoles.

Note the turn-around of the frequency shift at the last "magic" size.

CO^+He_n ground state densities from DMC

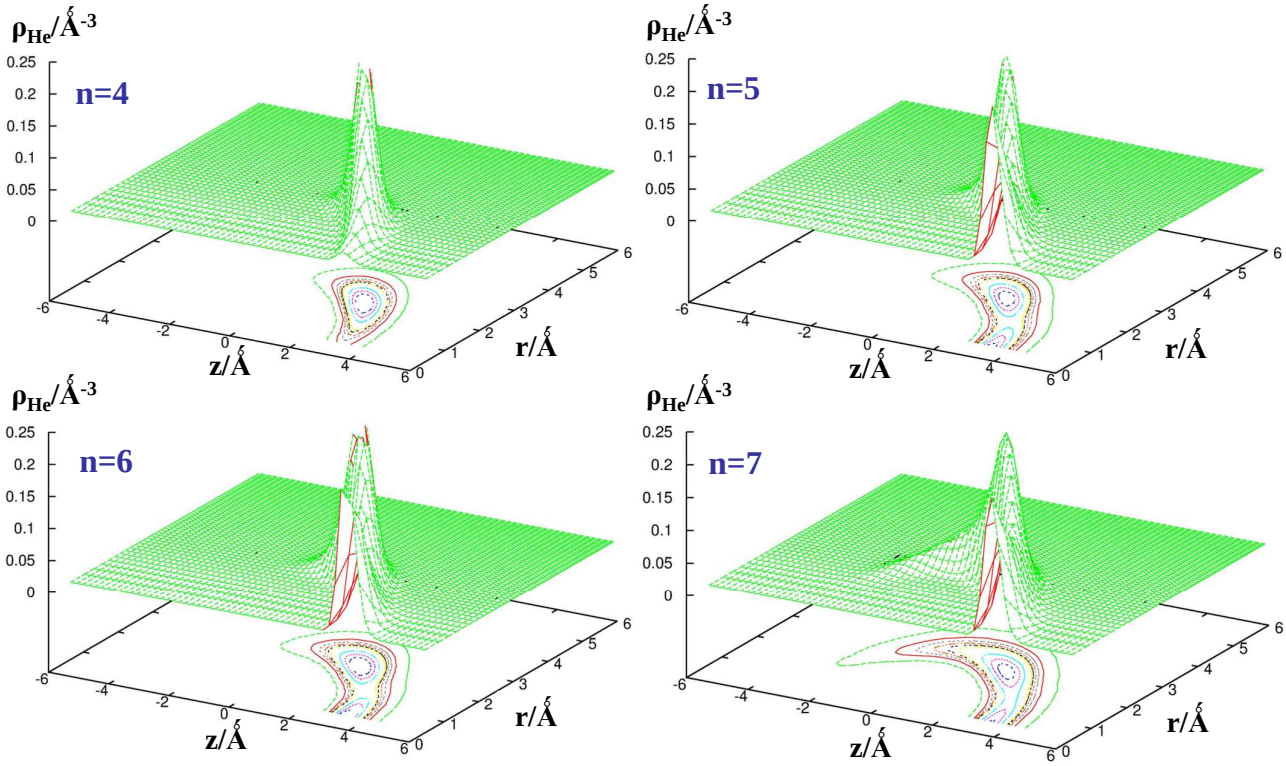

CO^+He_n DMC ground state densities:

build up of strongly anisotropic first helium shell

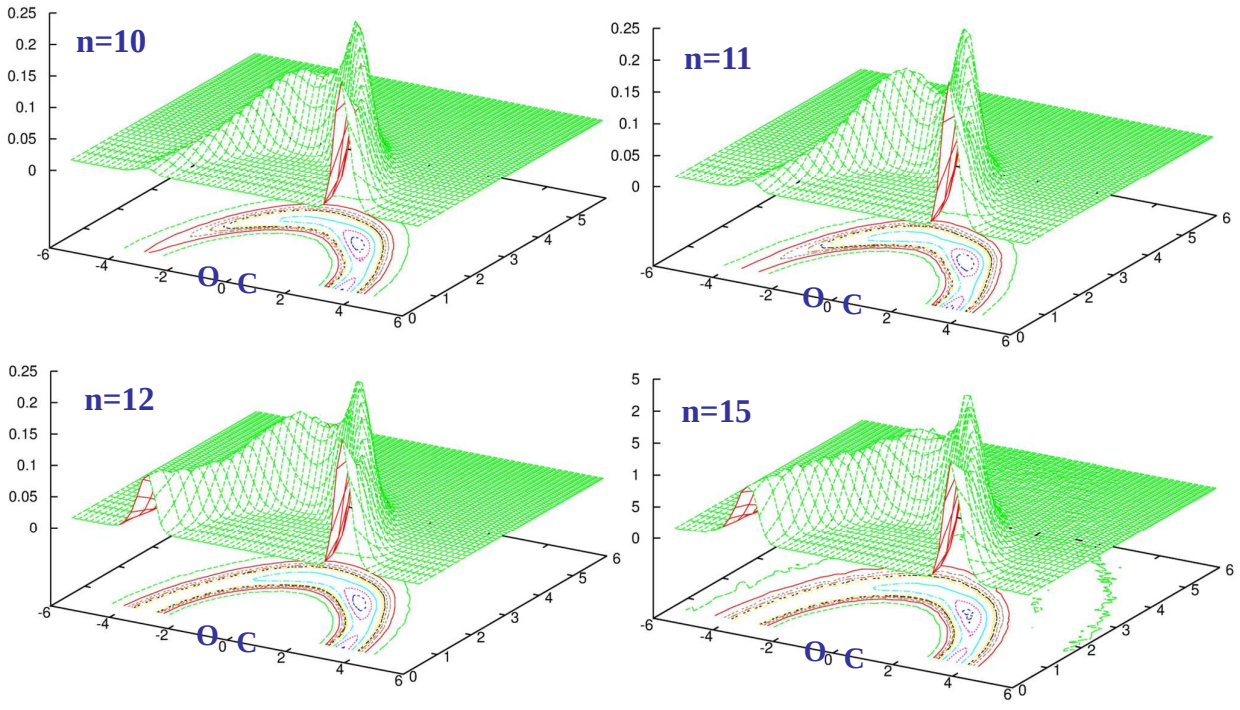

CO^+He_n DMC ground state densities:

onset of second helium shell at n=16

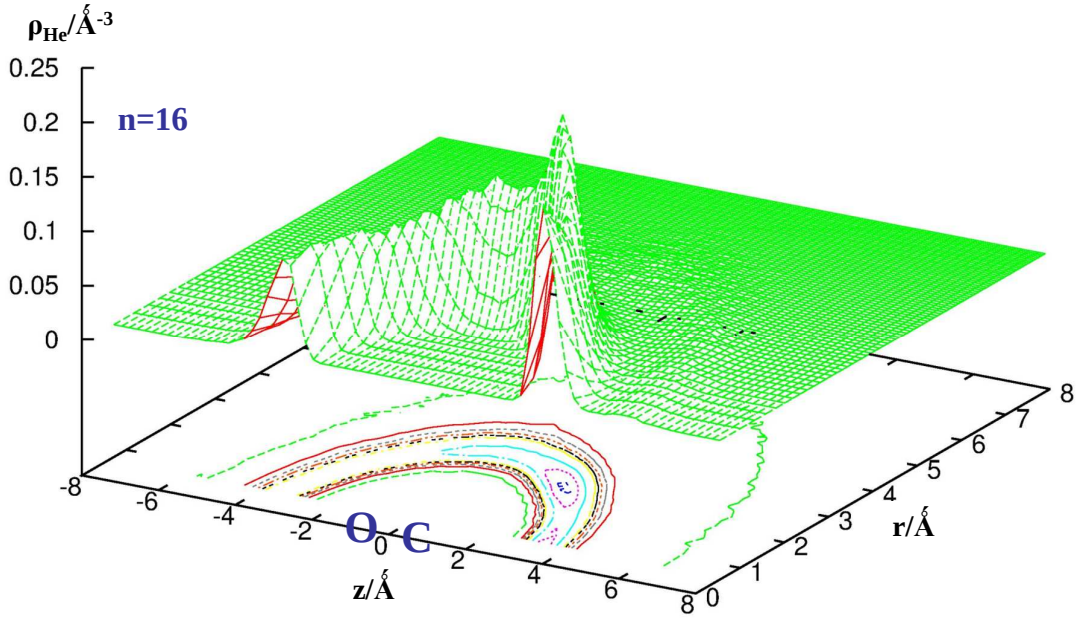

CO^+He_n DMC ground state densities:

build up of second helium shell

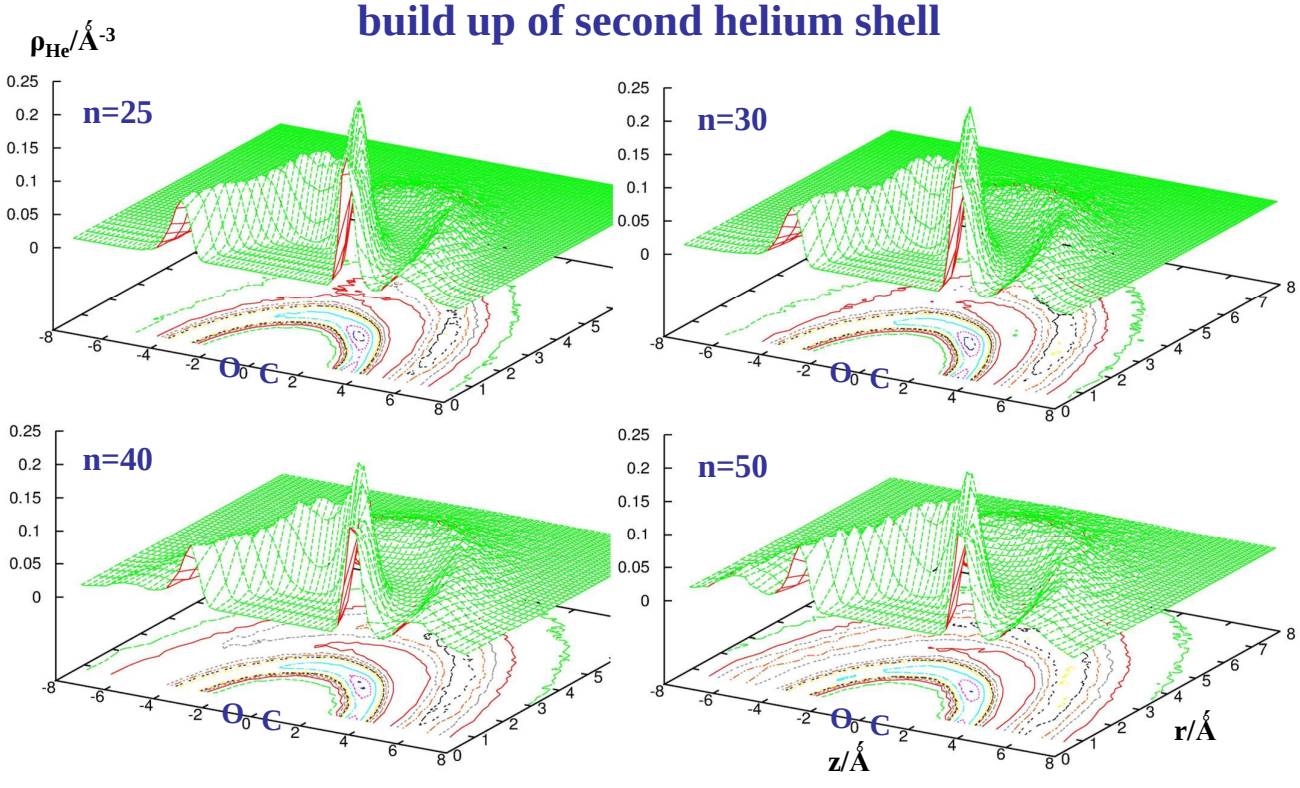

CH_3-He

- Ab initio RCCSD(T) calculations with aug-cc-pVXZ basis sets (X=D,T,Q,5)
- CH_3 keeping C_{3v} symmetry and fixed C-H distance: only umbrella angle α
- He position relative to CH_3 center of mass in spherical coordinates R,θ,φ
- Several 3D surfaces assembled into 4D surface including CH_3 relaxation
- Overall about 3000 potential energy points

Analytical representation with angle dependent HFD form expanded over real spherical harmonics T_{lm} with symmetry restrictions on l,m:

$$V(R,\theta,\varphi) = A \exp\{-b(\theta,\varphi)\,[R-R_e(\theta,\varphi)]\} - \Sigma_k\, C_k(\theta,\varphi)/R^k$$

$$X(\theta,\varphi) = \Sigma_{lm}\, x_{lm}\, T_{lm}(\theta,\varphi) \qquad X=b,\ R_e,\ C_k$$

500-1000 points per 3D cut are fitted with 38 parameters and rms < 0.1 cm^{-1}

Outlook

- Effective rotational constants for CO^+ in helium (DMC/PIMC in collaboration with P. N. Roy).
- CH_3 radicals in helium, reactive complexes.
- Photodissociation of CH_3I and CF_3I (ZPAD, DMC etc.)
- Dopant spectroscopy (Mg^*, Ag^*, Ag^+ etc.).
- Transport properties (Mg^+, Na^+).
- DMC and ZPAD calculations on Xe_nHe_m.
- DMC with constraints ($(H_2)_n$, $He_n(H_2)_m$ possible).
- SBDMC: soft body DMC allowing feedback between dopant and bath vibrations, quaternions for rotation.

ANR project DYNHELIUM (Toulouse, Rennes, Paris)